rhodium atom results in the formation of a four-membered RhSRhS ring with all Rh–S bond lengths nearly equal. The value of the S–S bond distance is 2.022 (3) Å. The same type of μ,η^2–η^1 bonding mode of the S_2 ligand occurs also in the disulfur complexes $[Mo_4(NO)_4S_{13}]^{4-}$,[8] $[Mo_2Fe_6S_{12}(S\text{-}p\text{-}(C_6H_4Br))]^{4-}$,[9] and $(\eta\text{-}C_5Me_5)_2Co_2S_4$,[10] which have close S–S distances [2.048 (7), 1.99 (5) and 2.062 (6) Å, respectively].

From a comparison between reaction paths 1 and 4, it is apparent that the elimination of CO is followed in both cases by the formation of new heterocyclic rings containing S–S or Se–Se bonds. While the dithiete decomposes to the dithiin, the Rh-η^2-X_2 (X = S, Se) rings, which belong to coordinatively and electronically unsaturated metal fragments, are stabilized by dimerization of the latter.

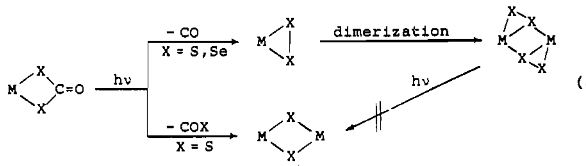

(4)

At variance with the reactions of organic dithiocarbonates, the inorganic analogues tend to lose also COS, a reaction pattern that, to a certain extent, resembles the photochemical decomposition of 4,5-diphenyl-1,2,3-dithiazole (eq 5).[11]

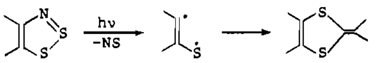

(5)

Supplementary Material Available: Fractional atomic coordinates and thermal parameters for compound **4** (4 pages). Ordering information is given on any current masthead page.

---

(8) Muller, A.; Eltzner, W.; Mohan, N. *Angew. Chem., Int. Ed. Engl.* **1979**, *8*, 168.

(9) Kovacs, J. A.; Bashkin, J. K.; Holm, R. H. *J. Am. Chem. Soc.* **1985**, *107*, 1784.

(10) Brunner, H.; Janietz, N.; Meier, W.; Sergerson, G.; Wachter, J.; Zahn, T.; Ziegler, M. *Angew. Chem., Int. Ed. Engl.* **1985**, *24*, 1060.

(11) Kirmse, W.; Horner, L. *Justus Liebigs Ann. Chem.* **1958**, *4*, 614.

Istituto per lo Studio della Stereochimica ed Energetica dei Composti di Coordinazione, CNR
50132 Florence, Italy
Claudio Bianchini*
Andrea Meli

Received November 13, 1986

Articles

Contribution from the Department of Chemistry,
University of Minnesota, Minneapolis, Minnesota 55455

Characterization of Large Cationic Transition-Metal–Gold Clusters by Fast Atom Bombardment Mass Spectroscopy (FABMS). New Re–Au and Pt–Au Clusters: $[Au_4Re(H)_4[P(p\text{-tol})_3]_2(PPh_3)_4]^+$, $[Au_2Re_2(H)_6(PPh_3)_6]^+$, and $[Au_6Pt(PPh_3)_7]^{2+}$.

Paul D. Boyle, Brian J. Johnson, Bruce D. Alexander, Joseph A. Casalnuovo, Patrick R. Gannon, Steven M. Johnson, Edmund A. Larka, Ann M. Mueting, and Louis H. Pignolet*

Received October 7, 1986

Fast atom bombardment mass spectroscopy has been used to examine a large number of cationic phosphine-containing transition-metal–gold clusters including polyhydrides, which ranged in mass from 1000 to 4000. Many of these clusters have been previously characterized and were examined in order to test the usefulness of the FABMS technique. Results showed that FABMS is excellent in giving the correct molecular formula including the number of hydride ligands, and when combined with NMR, conductance and analytical data gave complete and reliable characterization. Four new complexes have been synthesized and completely characterized by the above techniques. These are $[Au_2Pt(PPh_3)_4NO_3]NO_3$, $[Au_6Pt(PPh_3)_7](BPh_4)_2$, $[Au_2Re_2(H)_6(PPh_3)_6]PF_6$, and $[Au_4Re(H)_4[P(p\text{-tol})_3]_2(PPh_3)_4]PF_6$. The FABMS of these and other similar cationic and dicationic clusters with use of *m*-nitrobenzyl alcohol (MNBA) as the matrix always gave well-resolved peaks for either the parent molecular ion $(M)^+$ or the ion pair $(M + X)^+$ where X = the counterion. Comparison of observed and calculated isotopic ion distributions for these peaks reliably gave the correct molecular formulas. Cluster fragments were also observed that in general resulted from loss of one or more of the following species: PPh_3, H, CO, Ph, $AuPPh_3$. Small peaks that resulted from the addition of matrix fragments to unsaturated cluster ions were also observed. It is important to emphasize the necessity to compare the observed with the calculated isotopic ion distribution in order to accurately determine the formula of all cluster ions.

Introduction

Cationic transition-metal–gold clusters with predominantly phosphine ligands are a class of compounds of great current interest.[1-8] These compounds are important because of their novel structural features, because of their potential use as catalyst materials, and in understanding gold and gold alloy surface catalysis.[9,10] The characterization of such compounds has been a major problem in this area and generally has required the use of single-crystal X-ray crystallography. Since many of these clusters also contain hydride ligands, even crystallography has not always lead to a definitive answer, and of course it is often impossible

---

(1) Alexander, B. D.; Johnson, B. J.; Johnson, S. M.; Casalnuovo, A. L.; Pignolet, L. H. *J. Am. Chem. Soc.* **1986**, *108*, 4409 and references cited therein.

(2) Boyle, P. D.; Johnson, B. J.; Buehler, A.; Pignolet, L. H. *Inorg. Chem.* **1986**, *25*, 5.

(3) Gilmour, D. I.; Mingos, M. P. *J. Organomet. Chem.* **1986**, *302*, 127 and references cited therein.

(4) Briant, C. E.; Gilmour, D. I.; Mingos, D. M. P. *J. Chem. Soc., Dalton Trans.* **1986**, 835.

(5) Lehner, H.; Matt, D.; Pregosin, P. S.; Venanzi, L. M.; Albinati, A. *J. Am. Chem. Soc.* **1982**, *104*, 6825.

(6) Braunstein, P.; Lehner, H.; Tiripicchio, D. M. A.; Tiripicchio-Camellini, M. *Angew. Chem., Int. Ed. Engl.* **1984**, *23*, 304.

(7) Teo, B. K.; Keating, K. *J. Am. Chem. Soc.* **1984**, *106*, 2224.

(8) Melnik, M.; Parish, R. V. *Coord. Chem. Rev.* **1986**, *70*, 157.

(9) Schwank, J. *Gold Bull.* **1983**, *16*, 103.

(10) Sinfelt, J. H. *Bimetallic Catalysis*; Wiley: New York, 1983; Chapter 2. Wachs, I. E. *Gold Bull.* **1983**, *16*, 98.

0020-1669/87/1326-1346$01.50/0

to obtain X-ray quality crystals. The recent successful use of FABMS[11,12] in the characterization of ionic metal clusters[13-15] has prompted us to try this technique with cationic transition-metal–gold phosphine clusters including ones with hydride ligands. The results reported in this paper show that well-resolved spectra have been obtained for a large variety of such clusters and when combined with NMR and conductivity data will usually lead to an accurate determination of the molecular formula. Two new polyhydrido Re–Au clusters and a large Pt–Au cluster were synthesized in our lab some time ago, but their complete characterization had proved elusive and frustrating. The positive ion FABMS of these clusters gave peaks due to the parent ion and cluster fragments with well-resolved fine structure. An analysis of the isotopic ion distributions of these peaks clearly established the molecular formulas of the clusters, thus greatly advancing our research. It is important and significant that FABMS analysis combined with NMR and conductivity data will generally lead to rapid characterization of new clusters of this type without the need to carry out single-crystal X-ray determinations.

Experimental Section

Physical Measurements and Reagents. All FABMS experiments were carried out with use of a VG Analytical, Ltd., 7070E-HF high-resolution double-focusing mass spectrometer equipped with a VG 11/250 data system. A *m*-nitrobenzyl alcohol (MNBA) matrix was used, and experiments were run with a resolution of 4000. Ions (at accelerating potentials of 3 kV) were generated from impact on the target matrix of a neutral xenon atom beam derived from a Xe^+ ion beam at an accelerating potential of 8 kV. The FAB gun emission current was 1 mA. Spectra were analyzed by comparison to isotopic ion distributions calculated via the ISO program of VG Analytical, Ltd. For wide-scan conventional mass data, mass calibration was achieved with use of reference spectra of CsI clusters. Calibration was checked before and after acquisition of data with a maximum error of ± 0.3 Da. For the $[Au_2Re_2(H)_6(PPh_3)_6]PF_6$ cluster, the low mass ion in the ion distribution envelope (see Figure 4) has a unique atomic composition that corresponds to $^{185}Re_2{}^{197}Au_2{}^{31}P_6{}^{12}C_{108}{}^{1}H_{96}$. This ion has a calculated mass of 2342.4329. For the 2200–2500 mass range, 10 linear voltage scans at 3000 resolution at 20 s/scan were digitized and summed by the VG data system operating in a multichannel analyzer, signal-averaging mode. Reference spectra of CsI clusters in the same mass window were acquired in a similar manner and were used for mass calibration with use of peak-matching software in the data system. The observed mass for the low mass ion for two different samples was 2342.4524 and 2342.2495 and differed by an average of 43.3 ppm from the calculated value. A similar analysis for the $[Au_2Re_2(H)_7(PPh_3)_6]PF_6$ cluster (vide infra) gave calculated and observed mass values of 2343.4407 and 2343.3513, respectively, and a difference of 38.1 ppm. These results show that the molecular mass assignments are correct to within 100 ppm. ^1H and ^{31}P NMR spectra were recorded at 300 and 121.5 MHz, respectively, with the use of a Nicolet NT-300 spectrometer. ^{31}P NMR spectra were run with proton decoupling and are reported in ppm relative to the internal standard trimethyl phosphate (TMP), with positive shifts downfield. Infrared spectra were recorded on a Perkin-Elmer Model 281 grating spectrometer. UV–vis spectra were recorded with use of a Hewlett-Packard 8451 diode array spectrometer. Conductivity measurements were made with the use of a Yellow Springs Model 31 conductivity bridge. Magnetic susceptibility measurements were made by the Faraday technique with use of $Hg[Co(SCN)_4]$ as calibrant. Microanalyses were carried out by M-H-W Laboratories, Phoenix, AZ. All solvents were reagent grade and used as received, except for CH_3OH, which was distilled from magnesium turnings; CH_2Cl_2, which was distilled from P_2O_5; and THF, which was distilled from sodium benzophenone ketyl. $AuPPh_3NO_3$,[16] $Pt(PPh_3)_3$,[17] $Pt(PPh_3)_2(C_2H_4)$,[18] $Re_2H_8(PPh_3)_4$,[19] and $[Ir(H)_2(bpy)(PPh_3)_2]BF_4$[1] were prepared as described in the literature. All other transition-metal–gold clusters that are included have been reported elsewhere and are referenced as they appear and in Table I. All syntheses were carried out under a purified N_2 atmosphere with the use of standard Schlenk techniques unless otherwise noted.

Preparation of Compounds. **$[Au_2Pt(NO_3)(PPh_3)_4]NO_3$ ((1)NO_3).** $Pt(PPh_3)_2(C_2H_4)$ (0.185 g, 0.248 mmol) and $AuPPh_3NO_3$ (0.270 g, 0.518 mmol) were placed in a Schlenk flask to which about 15 mL of THF was added. Almost immediately a cream-colored precipitate formed. After about 1 h of stirring the precipitate was collected on a frit, washed with THF and diethyl ether and dried in vacuo. A yield of 0.40 g was obtained (92%). The addition of excess KPF_6 in methanol to a CH_2Cl_2 solution of the NO_3^- salt followed by reduction of the solution volume produced $[Au_2Pt(NO_3)(PPh_3)_4]PF_6$ in high yield. The analytical data reported below is for the PF_6^- salt. IR (KBr pellet): ν(bound NO_3) 1490, 1480, 1270 cm^{-1} (s); ν(P–F) 840 cm^{-1} (s). ^{31}P NMR (CH_2Cl_2, 22 °C): δ 28.8 (s with ^{195}Pt satellites, $^2J(^{195}Pt-P) = 804$ Hz, integral = 1), 22.6 (s with ^{195}Pt satellites, $^1J(^{195}Pt-P) = 2502$ Hz, integral = 1). ^{31}P NMR (CH_3CN, 22 °C): δ 34.0 (s with ^{195}Pt satellites, $^2J(^{195}Pt-P) = 718$ Hz, integral = 1), 21.6 (s with ^{195}Pt satellites, $J(^{195}Pt-P) = 2390$ Hz, integral = 1). Conductance (CH_3CN solution, 3.1×10^{-4} M): 184 cm^2 mho mol^{-1} (1:2 electrolyte). Anal. Calcd for $PtAu_2C_{72}H_{60}F_6NO_3P_5$: C, 46.87; H, 3.28; P, 8.39. Found: C, 46.52, H, 3.00; P, 8.08. Unit cell dimensions determination by X-ray crystallography at 23 °C with use of Mo Kα($\lambda = 0.710\,69$ Å) radiation (crystal grown from CH_2Cl_2–Et_2O by slow solvent diffusion and mounted on glass rod with epoxy): triclinic, $a = 12.295$ (9) Å, $b = 22.54$ (3) Å, $c = 13.303$ (8) Å, $\alpha = 89.86$ (8), $\beta = 113.21$ (6), $\gamma = 93.03$ (9)°, $V = 3389$ Å^3. The formulation of **1** was confirmed by FABMS (see Table I and Discussion). Compound **1** was also synthesized with use of $Pt(PPh_3)_3$ as the source of platinum. In this case the reaction was not as clean and $Au(PPh_3)_2^+$ was formed as a byproduct.

$[Au_6Pt(PPh_3)_7](BPh_4)_2$ (2). The NO_3^- salt of **1** (100 mg, 0.0567 mmol) was dissolved in 10 mL of CH_2Cl_2 and placed under 1 atm of H_2 with stirring. The color changed from yellow to a dark orange-brown in about 20 min. The solution was stirred under H_2 for about 1 h. Ether was added to precipitate a brown material. This product was collected on a frit, washed with Et_2O, and dried in vacuo. The solid was then redissolved in CH_2Cl_2, and a solution of $NaBPh_4$ (45 mg, 0.13 mmol) in 10 mL CH_3OH was added. The solution volume was reduced until a brown solid began to deposit. At this point the solution was allowed to stir overnight. The solid was collected on a frit, washed with CH_3OH and ether, and dried in vacuo. The yield was 45 mg (62%, based on Au). ^{31}P NMR (CH_2Cl_2, 22 °C): δ 50.2 (d with ^{195}Pt satellites, $J(P-P) = 30$ Hz, $^2J(^{195}Pt-P) = 413$ Hz), 62.3 (m, $J(P-P) = 30$ Hz)—see Discussion in text. ^1H NMR (acetone-d_6): δ 6.5–8.0 (m, aromatic H); no peaks in 0 to −30 ppm region. Conductance (CH_3CN solution, 2.9×10^{-4} M): 125 cm^2 mho mol^{-1} (1:2 electrolyte). The formulation of **2** was confirmed by FABMS (see Table 1 and Discussions).

$[Au_4Re(H)_4[P(p\text{-tol})_3]_2(PPh_3)_4]PF_6$ (3). $[Au_5Re(H)_4[P(p\text{-tol})_3]_2(PPh_3)_5](PF_6)_2$[2] (0.218 g, 0.0644 mmol, $P(p\text{-tol})_3$ is tri-*p*-tolylphosphine and is bound to the Re) and PPh_3 (0.0516 g, 0.197 mmol) were placed in a flask to which 7 mL of CH_2Cl_2 was added. The yellow solution was stirred for 12 h, and the solvent was then removed in vacuo. To the residue was added 5 mL of CH_3OH, which gave a suspension that was stirred and filtered through diatomaceous earth. CH_3OH was passed through the filter until the yellow color in the filtrate was no longer apparent (ca 20 mL). A yellow solid precipitated upon reduction of the volume of the CH_3OH solution. Crystallization from CH_2Cl_2–pentane produced yellow crystals in 56% yield. ^{31}P NMR (CH_2Cl_2, 25 °C): δ 53.2 (t, $J(P-P) = 6.7$ Hz, assigned as Au*P*), 23.7 (quin, $J(P-P) = 6.7$ Hz, assigned as Re*P*). ^1H NMR (CD_2Cl_2, 25 °C): δ −3.43 (9-line m; *t* with Au*P* decoupled, J(Re*P*–H) = 20.4 Hz; quin with Re*P* decoupled, J(Au*P*–H) = 8.5 Hz). Conductance (CH_3CN solution, 3×10^{-4} M): 60 cm^2 mho mol^{-1} (1:1 electrolyte). Unit cell dimensions determined by X-ray crystallography at 23 °C (Mo Kα, $\lambda = 0.710\,69$ Å): $a = 17.06$ (1) Å, $b = 28.09$ (1) Å, $c = 28.04$ (1) Å, $\alpha = 88.60$ (3), $\beta = 107.74$ (4), $\gamma = 89.99$ (5)°, $V = 12\,795$ Å^3. The formulation of **3** was confirmed by FABMS (see Discussion).

$[Au_2Re_2(H)_6(PPh_3)_6]X$ (4), X = PF_6 and BPh_4. $Re_2(H)_8(PPh_3)_4$ (0.150 g, 0.105 mmol) and $AuPPh_3NO_3$ (0.110 g, 0.211 mmol) were placed in a flask to which 7 mL of cold (−20 °C) CH_2Cl_2 was added. As this mixture was slowly warmed to room temperature, it changed from a red suspension to a red-brown solution and at about 0 °C to a dark green solution. After several minutes of stirring at room temperature, the CH_2Cl_2 solvent was pumped off. The remaining solid was dissolved in CH_3OH, and upon the addition of a methanol solution of 3 equiv of

---

(11) Miller, J. M. *J. Organomet. Chem.* **1983**, *249*, 299.

(12) Yergey, J.; Heller, D.; Hansen, G.; Cotter, R. J.; Fenselau, C. *Anal. Chem.* **1983**, *55*, 353. Jaitner, P.; Huber, W. *Inorg. Chim. Acta* **1986**, *111*, L11.

(13) Suslick, K. S.; Cook, J. C.; Rapko, B.; Droege, M. W.; Finke, R. G. *Inorg. Chem.* **1986**, *25*, 241.

(14) Henly, T. J.; Shapley, J. R.; Rheingold, A. I. *J. Organomet. Chem.* **1986**, *310*, 55.

(15) Davis, R.; Groves, I. F.; Durrant, J. L. A. *J. Organomet. Chem.* **1983**, *241*, C27.

(16) Malatesta, L.; Naldini, L.; Simonetta, G.; Cariati, F. *Coord. Chem. Rev.* **1966**, *1*, 255.

(17) Ugo, R.; Cariati, F.; La Monica, G. *Inorg. Synth.* **1968**, *11*, 105.

(18) Cook, C. D.; Jauhal, G. S. *J. Am. Chem. Soc.* **1968**, *90*, 1464.

(19) Chatt, J.; Coffey, R. S. *J. Chem. Soc. A* **1969**, 1963.

Table I. Positive Ion FABMS of Mixed Metal–Gold Clusters: Complex (M = Cluster Cation) Followed by *m/z*, Relative Abundance (Assignment)[a]

Complex	*m/z*	Relative Abundance	Assignment
$[Au_2Pt(PPh_3)_4NO_3]NO_3$ ((**1**)NO_3)	1700	35	$(M)^+$
	1638	82	$(M - NO_3)^+$
	1561	32	$(M - NO_3 - Ph)^+$
	1437	47	$(M - PPh_3)^+$
	1298	33	$(M - NO_3 - PPh_3 - Ph)^+$
	1221	100	$(M - NO_3 - PPh_3 - 2Ph)^+$
$[Au_6Pt(PPh_3)_7](BPh_4)_2$ (**2**)	3532	21	$(M + BPh_4)^+$
	3212	14	$(M)^+$
	2950	100	$(M - PPh_3)^+$
	2688	65	$(M - 2PPh_3)^+$
	2491	52	$(M - Au - 2PPh_3)^+$
	2194	49	$(M - 3PPh_3 - 3Ph)^+$
$[Au_4Re(H)_4[P(p\text{-}tol)_3]_2(PPh_3)_4]PF_6$ (**3**)	2781	3.7	$(M + PF_6)^+$
	2636	94	$(M)^+$
	2372	63	$(M - H - PPh_3)^+$
	2107	47	$(M - 4H - 2PPh_3)^+$
	1845	32	$(M - 4H - 3PPh_3)^+$
	1803	29	$(M - 4H - 2PPh_3 - P(p\text{-}tol)_3)^+$
	1729	51	$(M + PF_6 - 3H - 4PPh_3)^+$
	1583	51	$(M - 4H - 4PPh_3)^+$
	1541	100	$(M - 4H - 3PPh_3 - P(p\text{–}tol)_3)^+$
$[Au_2Re_2(H)_6(PPh_3)_6]PF_6$ (**4**)	2346	100	$(M)^+$
	1813[b]	43	$(M + 2H - Au - PPh_3 - Ph)^+$
	1736[b]	22	$(M + 2H - Au - PPh_3 - 2Ph)^+$
	1553[b]	30	$(M - 6H - 3PPh_3)^+$
	1475[b]	10	$(M - 6H - 3PPh_3 - Ph)^+$
	1291[b]	11	$(M - 6H - 4PPh_3)^+$
$[Au_5Re(H)_4[P(p\text{-}tol)_3]_2(PPh_3)_5](PF_6)_2$[2]	3240	5.3	$(M + PF_6 - H)^+$
	3162	1.3	$(M + PF_6 - H - Ph)^+$
	3096[b]	1.1	$(M)^+$
	3018[b]	0.8	$(M - H - Ph)^+$
	2636	100	$(M - Au - PPh_3)^+$
	2372	38	$(M - Au - H - 2PPh_3)^+$
$[AuIr(H)_2(bpy)(PPh_3)_3](BF_4)_2$[1]	1421	6.8	$(M + BF_4)^+$
	1334	2.3	$(M)^+$
	1072[b]	9.3	$(M - PPh_3)^+$
	875	100	$(M - Au - PPh_3)^+$
	667	12	$(M)^{2+}$
$[Ir(H)_2(bpy)(PPh_3)_2]BF_4$[1]	875[b]	100	$(M)^+$
	611	52	$(M - 2H - PPh_3)^+$
$[AuIr(H)(CO)(PPh_3)_4]PF_6$[1]	1467	0.8	$(M)^+$
	1205	100	$(M - PPh_3)^+$
	1175[c]	18	$(M - PPh_3 - CO - H)^+$
	1008	10	$(M - Au - PPh_3)^+$
	745	15	$(M - Au - 2PPh_3 - H)^+$
$[Au_2Ru(H)_2(dppm)_2(PPh_3)_2](PF_6)_2$[1]	1935	10	$(M + PF_6)^+$
	1789[b]	7.7	$(M - H)^+$
	1329	100	$(M - 2H - Au - PPh_3)^+$
	1263[c]	19	$(M - 2H - 2PPh_3)^+$
	1067	19	$(M - 2H - Au - 2PPh_3)^+$
	869[c]	78	$(M - 2H - 2Au - 2PPh_3)^+$
$[Au_3Rh(H)(CO)(PPh_3)_5]PF_6$[2]	2034[b]	2.0	$(M)^+$
	2005	0.3	$(M - H - CO)^+$
	1771[b]	100	$(M - PPh_3)^+$
	1588	14	$(M - H - CO - PPh_3 - 2Ph)^+$
	1479[c]	11	$(M - H - CO - 2PPh_3)^+$
	1403	12	$(M - H - CO - 2PPh_3 - Ph)^+$
	1206	12	$(M - Au - H - CO - 2PPh_3 - Ph)^+$
	1141	33	$(M - H - CO - 3PPh_3 - Ph)^+$
$[AuIr_3(dppe)_3(H)_6(NO_3)]BF_4$[d]	2036	94	$(M)^+$
	1974	94	$(M - NO_3)^+$
	1814	69	$(M - NO_3 - 2Ph - 6H)^+$
	1737	47	$(M - NO_3 - 3Ph - 6H)^+$
	1381	100	$(M - NO_3 - Au - dppe + 2H)^+$
$[Au_6(PPh_3)_6](NO_3)_2$[e]	2755	21	$(M)^+$
	2555	36	$(M + NO_3 - PPh_3)^+$
	2493	45	$(M - PPh_3)^+$
	2296	42	$(M - Au - PPh_3)^+$
	2230	42	$(M - 2PPh_3)^+$
	2033	80	$(M - Au - 2PPh_3)^+$
	1968	36	$(M - 3PPh_3)^+$
	1891	29,	$(M - 3PPh_3 - Ph)^+$
	1836	21	$(M - 2Au - 2PPh_3)^+$
	1771	100	$(M - Au - 3PPh_3)^+$
	1706	26	$(M - 4PPh_3)^+$

[a] The *m/z* is the mass of the most abundant ion in the observed isotopic distribution. Isotopic distributions have been simulated for the listed molecular formulas and agree within experimental error with the observed patterns. Peaks that involved fragments of the MNBA matrix are not included in the table. In general, peaks that are greater than 5% relative abundance and within 1000 mass units of the parent are included. In clusters that contain gold and PPh_3 major peaks due to $(AuPPh_3)^+$ (459) and $[Au(PPh_3)_2]^+$ (721) are observed. Small peaks were often present that were 16 mass units higher than these for cluster fragments. This was due to the addition of an oxygen atom from the matrix. [b] Overlapping peaks due to loss of additional hydrogens. [c] The calculated most abundant ion for this formula has a mass that is 1 unit greater than that observed. [d] Casalnuovo, A. L.; Pignolet, L. H.; van der Velden, J. W. A.; Bour, J. J.; Steggerda, J. J. *J. Am. Chem. Soc.* **1983**, *105*, 5957. [e] Briant, C. E.; Hall, K. P.; Mingos, D. M. P.; Wheeler, A. C. *J. Chem. Soc., Dalton Trans.* **1986**, 687.

$NaBPh_4$ or KPF_6 a precipitate formed. The solid product was filtered with diatomaceous earth, washed with a small amount of CH_3OH, and dissolved through the filter with CH_2Cl_2. Formation of a dark green precipitate in 62% yield occurred upon the addition of diethyl ether. Reprecipitation was carried out with use of CH_2Cl_2–Et_2O. The following characterization data is for the PF_6^- salt of **4**. Conductance (CH_3CN, 3×10^{-4} M): 79.1 cm^2 mho mol^{-1} (1:1 electrolyte). UV-vis (λ (nm), log ε): 612, 3.70; 458, 3.57; 335, 4.10; 270, 4.58; Magnetic data: gram susceptibility $\chi_g = -1.26 \times 10^{-8}$ cgsu g^{-1}, corrected molar susceptibility $\chi_M = 1.30 \times 10^{-3}$ cgsu mol^{-1}, magnetic moment $\mu = 1.77\ \mu_B$. Anal. Calcd for $Au_2Re_2C_{132}H_{116}BP_6$ (BPh_4^- salt): C, 59.48; H, 4.39; P, 6.97. Found: C, 59.19; H, 4.60 P, 6.63. The formulation of **4** was confirmed by FABMS (see Discussion).

Results and Discussion

Several heteronuclear cationic clusters of gold with platinum and rhenium have previously been synthesized and characterized by NMR spectroscopy and single-crystal X-ray analysis. Examples include $[Au_2PtCl(PEt_3)_2(PPh_3)_2]^+$,[6] $[AuPt_3(\mu\text{-}CO)_3\{P(C_6H_{11})_3\}_4]^+$,[20] $[Au_2Pt_2(PPh_3)_4(CNC_6H_3Me_2\text{-}2,6)_4]^{2+}$,[4] and $[Au_5Re(H)_4(PPh_3)_7]^{2+}$.[2] We have synthesized some new large cationic clusters of these metals but unfortunately were unable to obtain good quality single crystals. The usual characterization data such as NMR and IR spectroscopy, conductance, and elemental analysis failed to give unambiguous formulations. Fortunately, the use of FABMS resulted in reliable characterization, especially when combined with the other analytical data (vide infra).

Gold–Platinum Clusters. The reaction of $Pt(C_2H_4)(PPh_3)_2$ with 2 equivalents of $AuPPh_3NO_3$ gave the cationic cluster $[Au_2Pt(NO_3)(PPh_3)_4]^+$ (**1**) as a nitrate salt in high yield. Metathesis with KPF_6 gave **1** as a crystalline hexafluorophosphate salt. ^{31}P NMR (CH_2Cl_2) and IR spectroscopic analysis of **1** combined with conductivity and elemental analysis data clearly established it to be similar to the known and X-ray-structured compound $[Au_2PtCl(PEt_3)_2(PPh_3)_2]^+$ recently reported by Braunstein.[6] In **1** the nitrate ligand is bound to Pt [IR analysis (KBr): $\nu(NO_3)$ = 1490, 1480, and 1270 cm^{-1}], thus replacing the chloride in the Braunstein compound and presumably dissociated (conductivity Λ = 184 cm^2 mho mol^{-1}) giving a dicationic cluster. FABMS analysis of **1** as the PF_6^- salt clearly showed the parent molecular ion $(M)^+ = [Au_2PtNO_3(PPh_3)_4]^+$ and $[M - NO_3]^+$ with observed most abundant masses (*m/z* 1700.3 and 1638.4, respectively) within experimental error of the calculated values (*m/z* 1700 and 1638, respectively; vide infra and Table I).

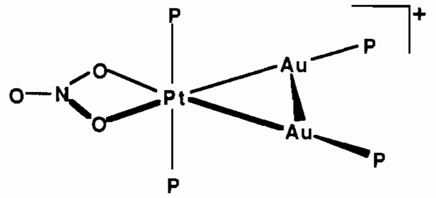

1

CH_2Cl_2 solutions of **1** changed in color from yellow to dark orange upon exposure to 1 atm of H_2, and a brown microcrystalline

---

(20) Mingos, D. M. P.; Wardle, R. W. M. *J. Chem. Soc., Dalton Trans.* **1986**, 73.

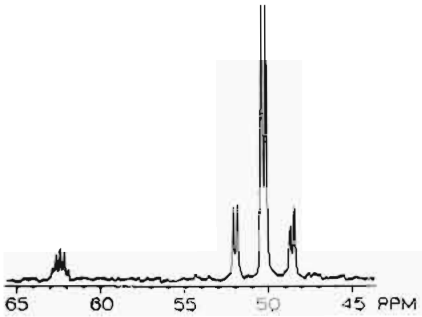

Figure 1. $^{31}P\{^1H\}$ NMR spectrum of $[Au_6Pt(PPh_3)_7](BPh_4)_2$ (**2**) recorded with use of CH_2Cl_2 as solvent at ambient temperature.

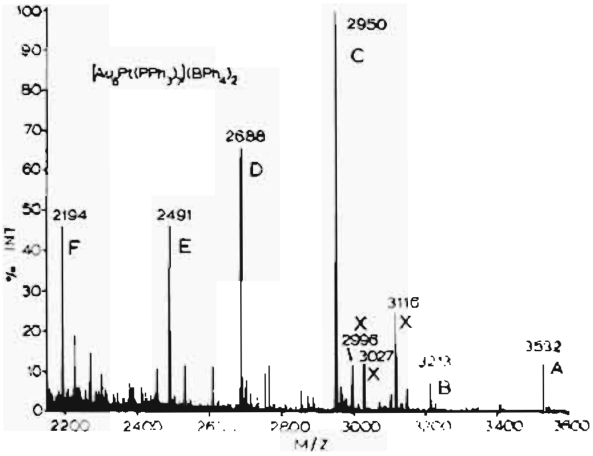

Figure 2. Positive ion FABMS (average of 10 scans) of $[Au_6Pt(PPh_3)_7](BPh_4)_2$ (**2**) in the *m/z* range 4000–2000, with a scan rate of 50 s/decade, 1:4000 resolution, and 3-kV accelerating voltage. The major peaks are assigned as follows where M = $[Au_6Pt(PPh_3)_7]$ and agree well with the calculated isotopic ion distribution patterns (see Figures 3 and 4): A, $(M + BPh_4)^+$; B, $(M)^+$; C, $(M - PPh_3)^+$; D, $(M - 2PPh_3)^+$; E, $(M - Au - 2PPh_3)^+$; F, $(M - 3PPh_3 - 3Ph)^+$. Peaks marked with an X have been assigned to cluster ions that incorporate fragments of the matrix MNBA (see text).

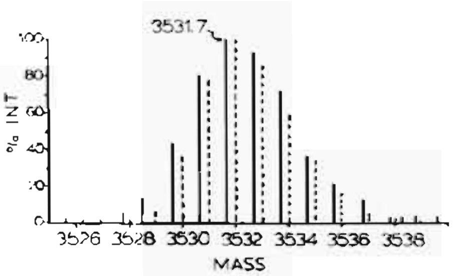

Figure 3. Observed (solid line) and simulated (dashed line) (VG ISO program) isotopic ion distributions for expanded peak A, $[Au_6PtP_7BC_{150}H_{125}]^+$, in the positive ion FABMS of $[Au_6Pt(PPh_3)_7](BPh_4)_2$ (**2**) shown in Figure 2.

solid was isolated after metathesis with $NaBPh_4$. This product did not show hydride signals in the ^1H NMR spectrum, and IR analysis indicated that coordinated nitrate was not present. The ^{31}P NMR (CH_2Cl_2) consisted of a large doublet (J(P–P) = 30 Hz) with ^{195}Pt satellites ($^2J(^{195}Pt-P)$ = 413 Hz) at δ 50.2 and a small multiplet (J(P–P) = 30 Hz) at δ 62.3 (Figure 1). ^{195}Pt satellites for the small peak were not observed due to its low intensity. Integration of the small multiplet vs. the central doublet gave a ratio of 1:6 ± 0.5. With this data it was not possible to reliably formulate the compound although it did appear that it was a large cluster with an approximate Au:Pt ratio of 6. Positive ion FABMS analysis of this compound gave a spectrum with well-resolved peaks that is shown in Figure 2. An analysis of the isotopic ion distribution pattern for the highest mass peak gave a most abundant mass ion of 3531.7. A complete simulation of all isotopic combinations for $[Au_6Pt(PPh_3)_7BPh_4]^+$ gave an isotopic ion distribution pattern that closely matched the observed pattern as shown in Figure 3. The calculated most abundant ion had *m/z* 3532 (Figure 3). Such a close comparison of the shape of the observed and calculated isotopic distributions provides good support for the assumed molecular formula.[12,13] An analysis of the fragmentation pattern shown in Figure 2 is given in the figure caption and in Table I (vide infra) and suggests that the neutral compound is $[Au_6Pt(PPh_3)_7](BPh_4)_2$ (**2**).[21] In agreement with this the conductance of **2** in CH_3CN showed it to be a 1:2 electrolyte. Support for the use of FABMS to characterize this type of cluster has been obtained by examining a large variety of known cationic mixed metal–gold clusters. These data are presented in Table I and will be discussed below.

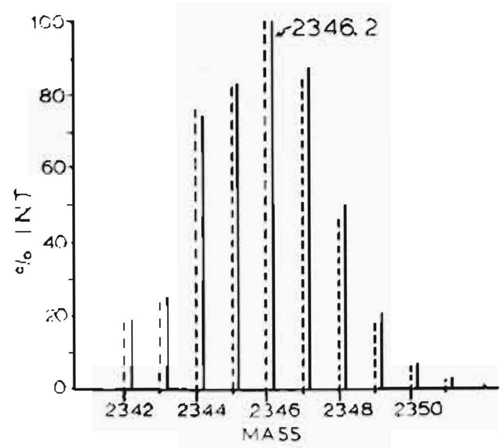

Figure 4. Observed (solid line) and simulated (dashed line) (VG ISO program) isotopic ion distributions for the $(M)^+$ cluster ion in the positive ion FABMS of $[Au_2Re_2(H)_6(PPh_3)_6]PF_6$ (**4**).

The formation of **2** from **1** by the reaction of H_2 is surprising although similar cluster growth reactions have been reported. For example, $[Au_3Ir(NO_3)(PPh_3)_5]^+$ reacts with H_2 to give $[Au_4Ir(H)_2(PPh_3)_6]^+$,[22] and H_2 is effective in reducing $AuPPh_3NO_3$ to $[Au_9(PPh_3)_8]^{3+}$ in ethanolic solution.[23] Work in progress is aimed at understanding this unusual reaction as well as examining other reactions of this and related Pt–Au clusters.

Gold–Rhenium Clusters. The reaction of $\{Au_5Re(H)_4[P(p\text{-}tol)_3]_2(PPh_3)_5\}(PF_6)_2$[2] with 3 equiv of PPh_3 in CH_2Cl_2 solution resulted in the formation of the new cluster $[Au_4Re(H)_4[P(p\text{-}tol)_3]_2(PPh_3)_4]PF_6$ (**3**) in good yield. The reaction involved the removal of a $(AuPPh_3)^+$ ion from the Au_5Re cluster and is apparently driven by the formation of $[Au(PPh_3)_2]^+$. This latter species was observed as a reaction product by ^{31}P NMR. The two $P(p\text{-}tol)_3$ ligands, P′, remained bound to the Re during the reaction. The structure of the $[Au_5Re(H)_4(PPh_3)_7]^{2+}$ cluster has been determined by X-ray crystallography and is shown in the drawing with P′ ligands. The hydride ligands were not located.[2]

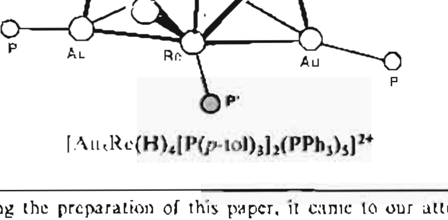

$[Au_5Re(H)_4[P(p\text{-}tol)_3]_2(PPh_3)_5]^{2+}$

---

(21) During the preparation of this paper, it came to our attention that Puddephatt has made and structurally characterized a similar Pt–Au cluster, $[Au_6Pt(C{\equiv}C\text{-}t\text{-}Bu)(PPh_3)_7]^+[Au(C{\equiv}C\text{-}t\text{-}Bu)_2]^-$. The NMR spectral data of the two clusters are similar, and the structure is that of two $PtAu_4$ square pyramids fused about a common face: Puddephatt, R. J., private communication.

(22) Casalnuovo, A. L.; Casalnuovo, J. A.; Nilsson, P. V.; Pignolet, L. H. *Inorg. Chem.* **1985**, *24*, 2554.

(23) Bos, W.; Bour, J. J.; Steggerda, J. J.; Pignolet, L. H. *Inorg. Chem.* **1985**, *24*, 4298.

The complete characterization of **3** was not straightforward due to problems in determining the number of hydride ligands. ^{31}P and ^{1}H NMR data (see Experimental Section) were entirely consistent with the $[(H)_xRe(P')_2(AuP)_4]^{n+}$ formulation but did not give values for *x* and *n*. The tetrahydrido formulation of the Au_5Re cluster was based on ^{1}H NMR integrations and is therefore also not 100% certain.[2] Fortunately, the positive ion FABMS analysis of both of these clusters gave direct evidence for the tetrahydrido compositions (see Table I and vide infra) and confirmed the original formulation of the Au_5Re cluster.[2] In **3** the major highest mass peak gave an isotopic ion distribution pattern which exactly matched that calculated for the parent cluster ion $[Au_4Re(H)_4P'_2P_4]^+$. The conductance of **3** showed it to be a 1:1 electrolyte in agreement with this formulation. The positive ion FABMS of other known and well-characterized polyhydrido mixed metal–gold clusters also showed species that contained the correct number of hydrides, thus demonstrating the reliability of this technique (vide infra).

The core geometry of **3** has been determined by single-crystal X-ray diffraction and is very similar to the core geometry of the Au_5ReP_7 cluster but with one of the wing-tip AuP fragments missing.[24] Reaction of **3** with 1 equiv of $AuPPh_3NO_3$ resulted in facile conversion back to the Au_5Re cluster, thus showing the reversible nature of these cluster interconversions.

The reaction of $Re_2(H)_8(PPh_3)_4$ with 2 equiv of $Au(PPh_3)NO_3$ in CH_2Cl_2 solution resulted in the formation of the new cationic cluster $[Au_2Re_2(H)_6(PPh_3)_6]^+$ (**4**), which was isolated in good yield as a PF_6^- or BPh_4^- salt. The compound is dark green in solution. Characterization of **4** was achieved by a combination of elemental analysis, conductance, magnetic susceptibility and FABMS. Single crystals could not be obtained, and the FABMS data were essential in the formulation of **4**, especially with regard to the number of hydride ligands. The major high mass peak in the positive ion FABMS was due to the parent cation $[Au_2Re_2(H)_6(PPh_3)_6]^+$ (see Table I). The isotopic ion distribution pattern of this peak agreed well with the simulated pattern (see Figure 4) thus confirming this formulation. The conductance was consistent with that of a 1:1 electrolyte, and the magnetic moment (1.77 μ_B) indicated the presence of one unpaired electron. This compound was always contaminated with a small amount of diamagnetic $[Au_2Re_2(H)_7(PPh_3)_6]^+$ as evidenced by ^{31}P and ^{1}H NMR. The identity of this compound was confirmed by comparison to an authentic sample kindly supplied by Walton and co-workers.[25] Compound **4** is the first dirhenium–gold compound thus far reported,[26] and work is under way to explore its rich acid–base chemistry and its electrochemistry.

FABMS of Mixed Metal–Gold Clusters. The results reported in the previous sections demonstrated the usefulness of positive ion FABMS in determining the formulation of several new cationic mixed metal–gold clusters including some that contained hydride ligands. In order to determine the generality of this technique, a number of well-characterized mixed metal–gold and related clusters have been examined and the results are reported in Table I. In all cases the spectra gave well-defined peaks, which could be readily assigned to cluster ions, similar to that shown in Figure 2. For ions in the 1000–4000 mass range, each peak consisted of a complex envelope as shown in Figures 3 and 4 due to the various isotopic combinations for a given molecular formula. It is absolutely necessary to calculate the isotopic ion combinations for each envelope and compare the shape to that of the observed distribution. In general, the mass of the most abundant mass ion (highest line in the envelope) is close to that calculated for the monoisotopic mass ion (calculated from the most abundant isotope of each element), but it can differ significantly and lead to an erroneous assignment. This is especially true for polyhydride clusters where differences of several mass units are important. Therefore, all of the peaks listed in Table I have been assigned by comparing theoretical with observed isotopic ion distributions as shown in Figures 3 and 4. The necessity of this for high mass ions has been discussed by others.[12,13]

The data shown in Table I and in Figures 2–4 lead to several important conclusions. For *monocationic clusters*, the $(M)^+$ ion was always observed [(M) is defined as the cluster without its anionic counter ions X]. For *dicationic clusters*, the $(M + X)^+$ ion pair was usually observed but anion loss was an important process and $(M)^+$ was also usually present; in all cases $(M)^+$ or $(M + X)^+$ was readily identified, giving the correct molecular formula. For *polyhydride clusters*, peaks were always present that corresponded to ions which contained *all* of the hydride ligands (for example, see Figure 4). Hydride loss was an important process, however, and often gave complicated overlapping isotopic distribution envelopes. It was important to compare theoretical isotopic distributions to the observed ones as shown in Figure 4 in order to confirm the molecular formula of the polyhydride cluster. Hydrogen addition to cluster ions did not occur, so true molecular formulas could be determined. However, hydrogen atom loss and addition are frequently observed processes in FABMS so care must be taken in determining the number of hydrogens present. It is important to consider the complete available data which should at least include conductance, NMR and magnetism. *Fragmentation patterns* included well-defined cluster ions that resulted from the loss of species such as phosphine, anion X, H, CO, phenyl, and $AuPPh_3$; the species $(AuPPh_3)^+$ and $[Au(PPh_3)_2]^+$ were always present. Fragments of the *m*-nitrobenzyl alcohol (MNBA) matrix such as $C_6H_4NO_2CH_2$, $C_6H_4NO_2CH_2O$, $C_6H_4NO_2$, $C_6H_4CH_2O$, and $C_6H_4CH_2$ often added to unsaturated cluster ions, giving a variety of relatively low intensity ions. Such adducts were not generally observed for the $(M)^+$ or $(M + X)^+$ ions, and when they were, their intensities were barely above background. Matrix additions are well-known in FABMS[11,27-29] and did not lead to significant complications with the clusters studied here. Small peaks were generally present that were 16 mass units higher than cluster fragments. This resulted from oxygen atom addition from the matrix and has been observed before in the FABMS of organometallic compounds.[29]

Although the FABMS of these mixed metal–gold clusters gave accurate information on the molecular formula, it is considered very important to also analyze other spectroscopic and analytical data. Only in this way can a reliable formulation be obtained. NMR will give information on the relative number of nonequivalent phosphine ligands, confirm the presence or absence of hydrides, and give possibilities for the relative number of hydrides. Conductance measurements will generally give the ionic charge on the cluster but only if the molecular weight is known. All of these data taken together should permit reliable characterization including the correct number of hydride ligands.

Acknowledgment. This work was supported by the National Science Foundation (Grant CHE-851923) and by the donors of the Petroleum Research Fund, administered by the American Chemical Society. The Johnson Matthey Co. is acknowledged for generous loans of $RhCl_3$, $IrCl_3$, and $HAuCl_4$. We also acknowledge the National Science Foundation for partial support of the VG Analytical mass spectrometer (Grant CHE-8403319). We are very grateful to Professors R. A. Walton and K. G. Caulton for sharing their unpublished results with us and for many helpful discussions.

---

(24) Results to be published elsewhere.

(25) Walton synthesized the dirhenium–gold compound $[Au_2Re_2(H)_7(PPh_3)_6]PF_6$ and has provided us with a sample. The FABMS of this compound is consistent with its heptahydride formulation (M^+ = 2347 for the most abundant ion; calculated M^+ = 2347 and see Experimental Section). The ^{31}P NMR (CH_2Cl_2, 25 °C) spectrum showed two singlet peaks at δ 67.0 and 29.6 that integrated in a 1:2 ratio. The ^{1}H NMR (CD_2Cl_2) spectrum showed a poorly resolved multiplet from −90 to +40 °C at about δ −3.1. These values agree well with those observed for the diamagnetic impurity present in samples of **4**. Report of the synthesis of this and related compounds: Moehring, G. A.; Fanwick, P. E.; Walton, R. A. submitted for publication in *Inorg. Chem.*

(26) Caulton has recently synthesized the neutral reduced form of **4** but with PMe_2Ph ligands on the Re atoms and has characterized it by single-crystal X-ray diffraction.

(27) Gower, J. L. *Biomed. Mass Spectrom.* **1985**, *12*, 191.

(28) Rinehart, K. L., Jr. *Science (Washington, D.C.)* **1982**, *218*, 254.

(29) Sharp, T. R.; White, M. R.; Davis, J. F.; Stang, P. J. *Org. Mass Spectrom.* **1984**, *19*, 107.